NATIONAL ADVISORY COMMITTEE FOR AERONAUTICS

TECHNICAL NOTE 2009

THEORETICAL CALCULATIONS OF THE SUPERSONIC PRESSURE DISTRIBUTION AND WAVE DRAG FOR A LIMITED FAMILY OF TAPERED SWEPTBACK WINGS WITH SYMMETRICAL PARABOLIC-ARC SECTIONS AT ZERO LIFT

By Julian H. Kainer

Langley Aeronautical Laboratory
Langley Air Force Base, Va.

Washington
January 1950

NATIONAL ADVISORY COMMITTEE FOR AERONAUTICS

TECHNICAL NOTE 2009

THEORETICAL CALCULATIONS OF THE SUPERSONIC PRESSURE DISTRIBUTION AND WAVE DRAG FOR A LIMITED FAMILY OF TAPERED SWEPTBACK WINGS WITH SYMMETRICAL PARABOLIC-ARC SECTIONS AT ZERO LIFT

By Julian H. Kainer

SUMMARY

The study of the supersonic pressure distribution and wave drag of sweptback wings at zero lift has been extended by means of linearized theory to include the combined effects of plan-form taper and curvature of profile. Calculations have been made for a specific wing with a supersonic leading edge and these results are applicable to a limited family of plan forms. Comparisons have been made of the pressure distributions and the wave drag calculated by this exact linear solution with the results of an arbitrary simplified approximation based on formulas for untapered plan forms with symmetrical parabolic-arc sections. In addition, a comparison of the wing wave-drag coefficient has been made with the results obtained from formulas for geometrically similar sweptback tapered wings with rhombic sections modified by a profile-correction factor.

INTRODUCTION

During the past few years, extensive investigations utilizing linearized theory have been in progress to predict the aerodynamic characteristics of a wide variety of wing configurations at supersonic speeds. The method of reference 1 was applied for the case of zero lift in references 2 and 3 to predict the wave-drag characteristics of untapered sweptback wings with symmetrical parabolic-arc sections and in references 4 and 5 to predict the wave drag of tapered sweptback wings with rhombic profiles (symmetrical double-wedge sections with maximum thickness at the midchord). Reference 6 considered the effect of chordwise location of maximum thickness on the supersonic wave drag of sweptback wings with symmetrical double-wedge profiles. Since many practical configurations include combined plan-form taper and curvature of profile, it is of current interest to investigate this case. This

paper supplements the investigations of references 1 to 5 by presenting the calculations for the pressure distribution for a limited family of tapered sweptback plan forms with symmetrical parabolic-arc sections and supersonic leading edges at zero lift.

SYMBOLS

x, y, z	Cartesian coordinates with origin located at wing apex
ξ, η	coordinates of origin of source line
V	free-stream velocity in x-direction
M	free-stream Mach number
ϕ_x	first partial derivative of disturbance-velocity potential in x-direction
$\phi_{xx}, \phi_{yy}, \phi_{zz}$	second partial derivatives of disturbance-velocity potential in x-, y-, and z-directions, respectively
$\beta = \sqrt{M^2 - 1}$	
Λ	sweep of leading edge
b	wing span
c_r	root chord
c_t	tip chord
λ	taper ratio (c_t/c_r)
x_i, y_i	coordinates of intersection of extended leading and trailing edges
c	local chord in x-direction $\left(c_r\left(1 - \frac{y}{y_i}\right)\right)$
S	wing area
A	aspect ratio (b^2/S)
dz/dx	slope of airfoil surface
m	slope of source line $\left(\frac{y_i}{x_i - \xi}\right)$

$m_0 = \cot \Lambda$

t/c	thickness ratio
I	source-strength factor
u	horizontal perturbation velocity (ϕ_x in x,y-plane)
$\bar{u}$	u caused by source line with reversal in sign of y
$u_{\xi,\eta}$	u caused by source line originating at point (ξ,η)
$1/D$	integration operator
P	pressure coefficient $\left(-\frac{2}{V}\sum u\right)$
c_d	section wave-drag coefficient
C_D	wing wave-drag coefficient
R.P.	real part of complex expression

Subscripts used with u and $\bar{u}$ indicate origin of source line.

ANALYSIS

General Considerations

Within the assumptions of small disturbances, the linearized equation for the velocity potential is

$$(1 - M^2)\phi_{xx} + \phi_{yy} + \phi_{zz} = 0 \tag{1}$$

Because of the linearity of equation (1) a solution may be used to denote one of the velocity components rather than the velocity potential. (See reference 7.) The specification of one component in this manner actually describes the whole flow field since the other components may be obtained by integrating the given component to obtain the velocity potential and then differentiating the results along the desired directions to obtain the desired components. It was shown in reference 1 that a solution to equation (1) corresponding to a disturbance velocity at $z = 0$ of an oblique line of pressure sources in the plane $z = 0$ is, for $m\beta > 1.0$, equivalent to

$$u = \text{R.P.}\left[I \cos^{-1} \frac{x - m\beta^2 y}{\beta(mx - y)}\right] \tag{2}$$

and for $m\beta < 1.0$,

$$u = \text{R.P.}\left[I \cosh^{-1} \frac{x - m\beta^2 y}{\beta\left|y - mx\right|}\right] \tag{3}$$

where

$$I = \frac{V}{\pi} \frac{m}{\sqrt{\pm\left(m^2\beta^2 - 1\right)}} \frac{dz}{dx} \tag{4}$$

The + and - signs in equation (4) refer to equations (2) and (3), respectively. The origin of the lines of sources described in equations (2) and (3) is the origin of the coordinate system. Equations (2) to (4) were given in references 2 and 3 for a line of sources with origin located at any point (ξ,η) in another form and are for the supersonic leading edge $(m\beta > 1)$

$$u_{\xi,\eta}(x,y) = \text{R.P.}\left[I \cos^{-1} \frac{x - \xi - m\beta^2(y - \eta)}{\beta\left[m(x - \xi) - (y - \eta)\right]}\right] . \tag{5}$$

and for subsonic leading edge $(m\beta < 1)$

$$u_{\xi,\eta}(x,y) = \text{R.P.}\left[I \cosh^{-1} \frac{x - \xi - m\beta^2(y - \eta)}{\beta\left|m(x - \xi) - (y - \eta)\right|}\right] \tag{6}$$

where for an untapered wing $m = \cot \Lambda$ and for a tapered wing

$$m = \frac{y_i}{x_i - \xi} \tag{7}$$

In reference 1, the following is stated: "Curved surfaces require a continuous distribution of sources and sinks alined with the generators of the surface. Each elementary source line causes an infinitesimal change in direction of the surface and hence the slope at any point may be obtained by adding up the effects of all sources ahead of that point." Thus, it was shown (reference 1) that

$$\frac{dz}{dx} = \frac{\pi}{V} \int_{x_i}^{x} \frac{\sqrt{\pm(m^2\beta^2 - 1)}}{m} \frac{dI}{d\xi}\, d\xi \tag{8}$$

and

$$\frac{dI}{d\xi} = \frac{V}{\pi} \frac{m}{\sqrt{\pm\left(m^2\beta^2 - 1\right)}} \frac{d^2z}{d\xi^2} \tag{9}$$

Pressure Distribution

The pressure coefficient is given by

$$P = -\frac{2}{V}\sum u \tag{10}$$

where the summation in equation (10) represents the superposition of the finite sources of strength sufficient to form the desired angle of intersection of the arcs of the leading and trailing edges together with a continuous distribution of infinitesimal sources and sinks along the chord line to produce any desired curvature.

The following equations from references 3 and 2, respectively, when applied to wing plan forms where each tip affects solely its own half of the wing can be given as follows: For a supersonic leading edge ($m_0\beta > 1$)

$$\sum u = u_{0,0} + \bar{u}_{0,0} - \frac{1}{D}u_{0,0} - \frac{1}{D}\bar{u}_{0,0} - u_{b/2m_0,b/2} + \frac{1}{D}\bar{u}_{b/2m_0,b/2} \tag{11}$$

and for a subsonic leading edge ($m_0\beta < 1$)

$$\sum u = u_{0,0} + \bar{u}_{0,0} + u_{c,0} + \bar{u}_{c,0} - \frac{1}{D}u_{0,0} - \frac{1}{D}\bar{u}_{0,0} + \frac{1}{D}u_{c,0} + \frac{1}{D}\bar{u}_{c,0} - u_{b/2m_0,b/2} + \frac{1}{D}u_{b/2m_0,b/2} \tag{12}$$

where the unbarred quantities in equations (11) and (12) refer to contributions of the sources in the half-wing where the point under consideration is located, and the barred quantities refer to the contributions of those sources in the other half-wing, the disturbances of which are propagated to that point. The continuous distributions of sources and sinks (represented by $\frac{1}{D}u$ and $\frac{1}{D}\bar{u}$) in equations (11) and (12) are obtained by chordwise integration of the solution for an elementary line source given by the expression:

$$u_{\xi,\eta}(x,y) + \bar{u}_{\xi,\eta}(x,y) = \text{R.P.}\left[2I \cos^{-1}\frac{1}{\beta}\sqrt{\frac{(x-\xi)^2 - \beta^2(y-\eta)^2}{m^2(x-\xi)^2 - (y-\eta)^2}}\right] \tag{13}$$

The following formulas can be used to evaluate the contributions of the various terms of equations (11) and (12): For $m_0\beta > 1$

$$u_{0,0}(x,y) + \bar{u}_{0,0}(x,y) = \text{R.P.}\left[2I \cos^{-1}\frac{1}{\beta}\sqrt{\frac{x^2 - \beta^2y^2}{m^2x^2 - y^2}}\right] \tag{14}$$

For $m_0\beta < 1$

$$u_{0,0}(x,y) + \bar{u}_{0,0}(x,y) = \text{R.P.}\left[I\left[\cosh^{-1}\frac{x - m_0\beta^2 y}{\beta|m_0 x - y|} + \cosh^{-1}\frac{x + m_0\beta^2 y}{\beta(m_0 x + y)}\right]\right] \tag{15}$$

For the region ahead of the Mach line from the wing apex ($x \leq \beta y$ and $m_0\beta > 1$)

$$\frac{1}{D}u_{0,0}(x,y) + \frac{1}{D}\bar{u}_{0,0}(x,y) = \frac{V}{\beta}\int_{\xi=\frac{y}{m_0}}^{\xi=x}\frac{\frac{d^2z}{d\xi^2}\,d\xi}{\sqrt{1 - \left(\frac{1}{m\beta}\right)^2}} \tag{16}$$

The contributions $\left(\frac{1}{D}u + \frac{1}{D}\bar{u}\right)$ of the chordwise distributions of source and sink lines are obtained by a summation of the effects of all the elementary source and sink lines, the disturbances of which are propagated to the point (x,y). For instance, in the region between the leading edge and the Mach line from the wing apex (equation (16)) the contributions of the leading-edge source lines is $I\pi$, and the increment due to the change in source strength from an infinitesimal source line to another approaches $\pi\,dI$ in the limit. In the limit, the summation becomes an integration over the proper limits of $\pi\int dI$ or $\pi\int\frac{dI}{d\xi}\,d\xi$ along the root chord. For the region behind the Mach line from the wing apex ($x \geq \beta y$ and $m_0\beta > 1$)

$$\frac{1}{D}u_{0,0}(x,y) + \frac{1}{D}\bar{u}_{0,0}(x,y) = \frac{V}{\beta}\int_{\xi=\frac{y}{m_0}}^{\xi=\beta y}\frac{\frac{d^2z}{d\xi^2}\,d\xi}{\sqrt{1 - \left(\frac{1}{m\beta}\right)^2}} +$$

$$\frac{2V}{\pi\beta}\int_{\xi=0}^{\xi=x-\beta y}\frac{\frac{d^2z}{d\xi^2}\cos^{-1}\frac{1}{\beta}\sqrt{\frac{(x-\xi)^2 - \beta^2 y^2}{m^2(x-\xi)^2 - y^2}}}{\sqrt{1 - \left(\frac{1}{m\beta}\right)^2}}\,d\xi \tag{17}$$

where m is a function of ξ given by equation (7). The first term in equation (17) is the contribution of the elementary source lines from the leading edge to the Mach line emanating from the wing apex, and the last term represents the contribution of the elementary source lines between the Mach line from the wing apex and the forward Mach line of the point (x,y). For a subsonic leading edge ($m_0\beta < 1$)

$$\frac{1}{D}u_{0,0}(x,y) + \frac{1}{D}\bar{u}_{0,0}(x,y) = \left\{ \int_{\xi=0}^{\xi=x-\beta y} \frac{\frac{d^2z}{d\xi^2} \cosh^{-1} \frac{x - \xi - m\beta^2 y}{\beta\left|m(x - \xi) - y\right|}}{\sqrt{\left(\frac{1}{m\beta}\right)^2 - 1}} d\xi + \right.$$

$$\left. \int_{\xi=0}^{\xi=x-\beta y} \frac{\frac{d^2z}{d\xi^2} \cosh^{-1} \frac{x - \xi + m\beta^2 y}{\beta\left[m(x - \xi) + y\right]}}{\sqrt{\left(\frac{1}{m\beta}\right)^2 - 1}} d\xi \right\} \quad (18)$$

where equations (16) to (18) were given in another form in reference 1.

In calculations for a parabolic-arc section in the stream direction, $d^2z/d\xi^2$ is constant and may be removed from the integrands of equations (16) to (18). Because of the complexity of the integrations (equations (16) to (18)) for the contribution of combined plan-form taper and curvature of profile to the pressure distribution, graphical integration was considered the most advantageous means of obtaining the results.

Drag

Since the pressure distribution (equation (10)) for the tapered configuration was not available in closed form, the section wave-drag coefficients and the wing wave-drag coefficient were calculated by graphical means from the equations:

$$c_d = 2 \int_0^1 P \frac{dz}{dx} d\frac{x}{c} \quad (19)$$

where

$$\frac{dz}{dx} = 4\frac{t}{c}\left(\frac{1}{2} - \frac{x}{c}\right) \tag{20}$$

and

$$C_D = \frac{2}{1+\lambda}\int_0^1 c_d \frac{c}{c_r}\, d\frac{2y}{b} \tag{21}$$

RESULTS AND DISCUSSION

Pressure-distribution calculations have been made for the wing configuration of figure 1 having a symmetrical parabolic-arc section. The chordwise pressure distributions at the root chord, tip chord, and four intermediate spanwise stations are presented in figure 2. The distribution of section wave-drag coefficient (equation (19)) is shown in figure 3 and was integrated graphically (equation (21)) to give the wing wave-drag coefficient $C_D = 5.34(t/c)^2$ for the wing configuration of figure 1 or $C_D = 4.86(t/c)^2 \cot \Lambda$ for a limited family of tapered-wing configurations with symmetrical parabolic-arc sections satisfying $\lambda = 0.531$, $A\beta = 4.65$, and $\beta \cot \Lambda = 1.375$.

As a point of interest, the pressure distributions were calculated for the previously mentioned stations by an arbitrary approximation and are presented in figure 2; the pressure distribution at each station was calculated by the formulas of reference 1 for untapered wings having the same span and leading-edge sweep as the tapered wing and having a constant chord equal to the local chord of the tapered wing at the spanwise station under consideration. The untapered wings used in these computations are illustrated in figure 4. Although the results compare favorably in the vicinity of the root chord, the agreement becomes poor with distance from the root chord. (See fig. 2.)

The distribution of section wave-drag coefficient, also calculated with the use of the geometric assumptions indicated by figure 4 and the formulas of reference 3, is shown in figure 3. The corresponding wing wave-drag coefficient is $C_D = 5.29(t/c)^2 \cot \Lambda$, which is about 9 percent higher than the result of this paper.

The wing wave-drag coefficient calculated in the present paper ($C_D = 4.86(t/c)^2 \cot \Lambda$) was compared with the value obtained for a geometrically similar wing with rhombic profile (reference 5) multiplied

by a profile-correction factor. This factor was chosen as the ratio of the wing wave-drag coefficients of two untapered wings (having the same aspect ratio and leading-edge sweep as the tapered wing) with parabolic-arc (reference 3) and rhombic sections (reference 6), respectively. The wing wave-drag coefficient $C_D = 4.85(t/c)^2 \cot \Lambda$ so obtained when $A\beta = 4.65$ and $\beta \cot \Lambda = 1.375$ compared excellently with the value calculated herein.

CONCLUDING REMARKS

The study of the supersonic pressure distribution and wave drag of sweptback wings at zero lift has been extended by means of linearized theory to include the combined effects of plan-form taper and curvature of profile. Calculations have been made for a specific wing with a supersonic leading edge and these results are applicable to a limited family of plan forms. Comparisons have been made of the pressure distributions and the wave drag calculated by this exact linear solution with the results of an arbitrary simplified approximation based on formulas for untapered plan forms with symmetrical parabolic-arc sections. It appears that these approximations are adequate only in the vicinity of the root chord. In addition, the wing wave-drag coefficient was compared with a value obtained from that of a geometrically similar sweptback tapered plan form with a rhombic profile by using as a profile-correction factor the ratio of the wing wave-drag coefficients of two untapered wings (having the same aspect ratio and leading-edge sweep as the tapered wing) with parabolic-arc and rhombic sections, respectively. This approximation indicated excellent agreement for the cases considered.

Langley Aeronautical Laboratory
National Advisory Committee for Aeronautics
Langley Air Force Base, Va., November 1, 1949

REFERENCES

1. Jones, Robert T.: Thin Oblique Airfoils at Supersonic Speed. NACA Rep. 851, 1946.

2. Harmon, Sidney M., and Swanson, Margaret D.: Calculations of the Supersonic Wave Drag of Nonlifting Wings with Arbitrary Sweepback and Aspect Ratio. Wings Swept behind the Mach Lines. NACA TN 1319, 1947.

3. Harmon, Sidney M.: Theoretical Supersonic Wave Drag of Untapered Sweptback and Rectangular Wings at Zero Lift. NACA TN 1449, 1947.

4. Margolis, Kenneth: Supersonic Wave Drag of Sweptback Tapered Wings at Zero Lift. NACA TN 1448, 1947.

5. Margolis, Kenneth: Supersonic Wave Drag of Nonlifting Sweptback Tapered Wings with Mach Lines behind the Line of Maximum Thickness. NACA TN 1672, 1948.

6. Margolis, Kenneth: Effect of Chordwise Location of Maximum Thickness on the Supersonic Wave Drag of Sweptback Wings. NACA TN 1543, 1948.

7. Lamb, Horace: Hydrodynamics. Sixth ed., Cambridge Univ. Press, 1932, paragraph 37.

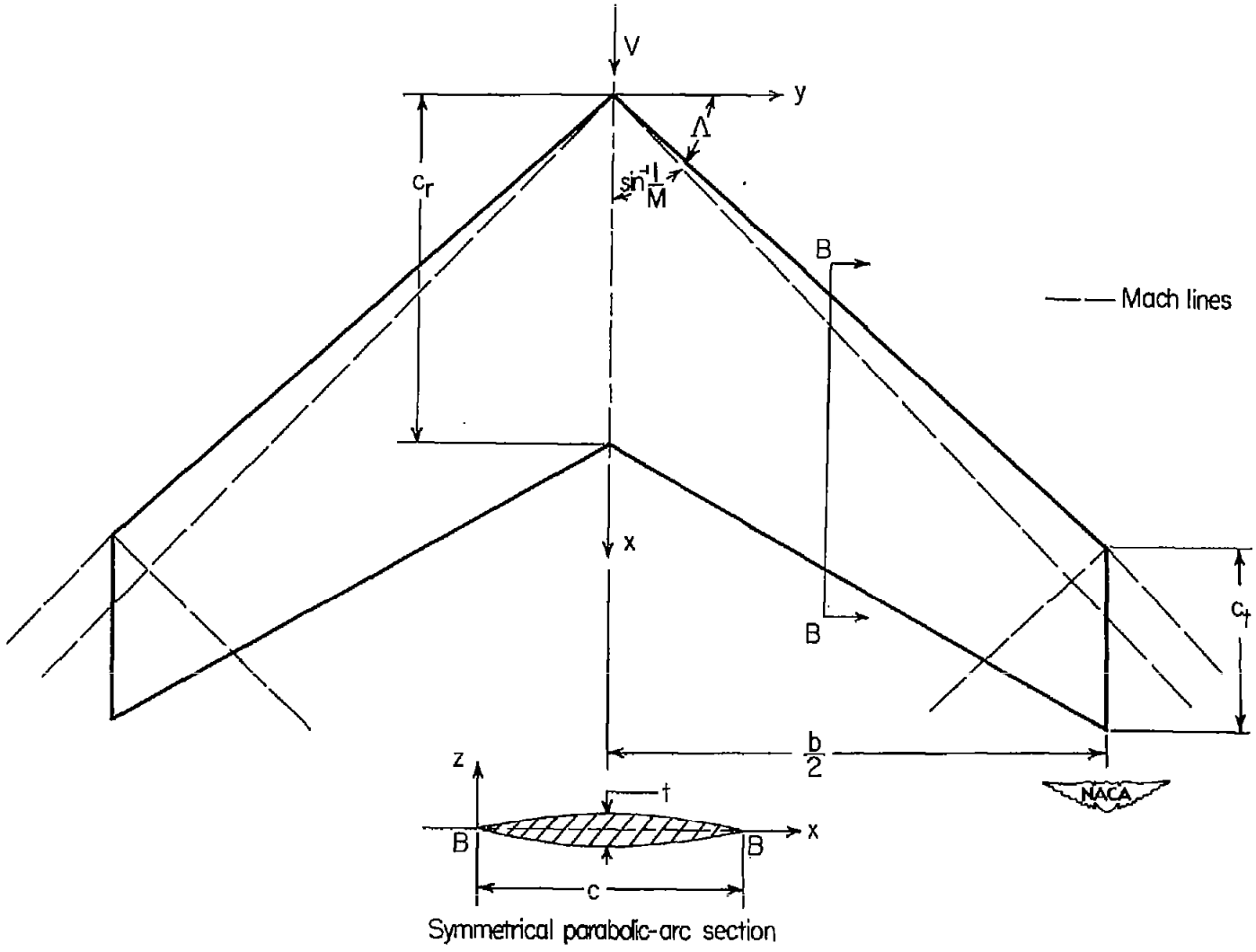

Figure 1.- Tapered-wing configuration with supersonic leading edges; A = 3.72, $\Lambda = 42.3^\circ$, $\lambda = 0.531$, and $M = 1.6$.

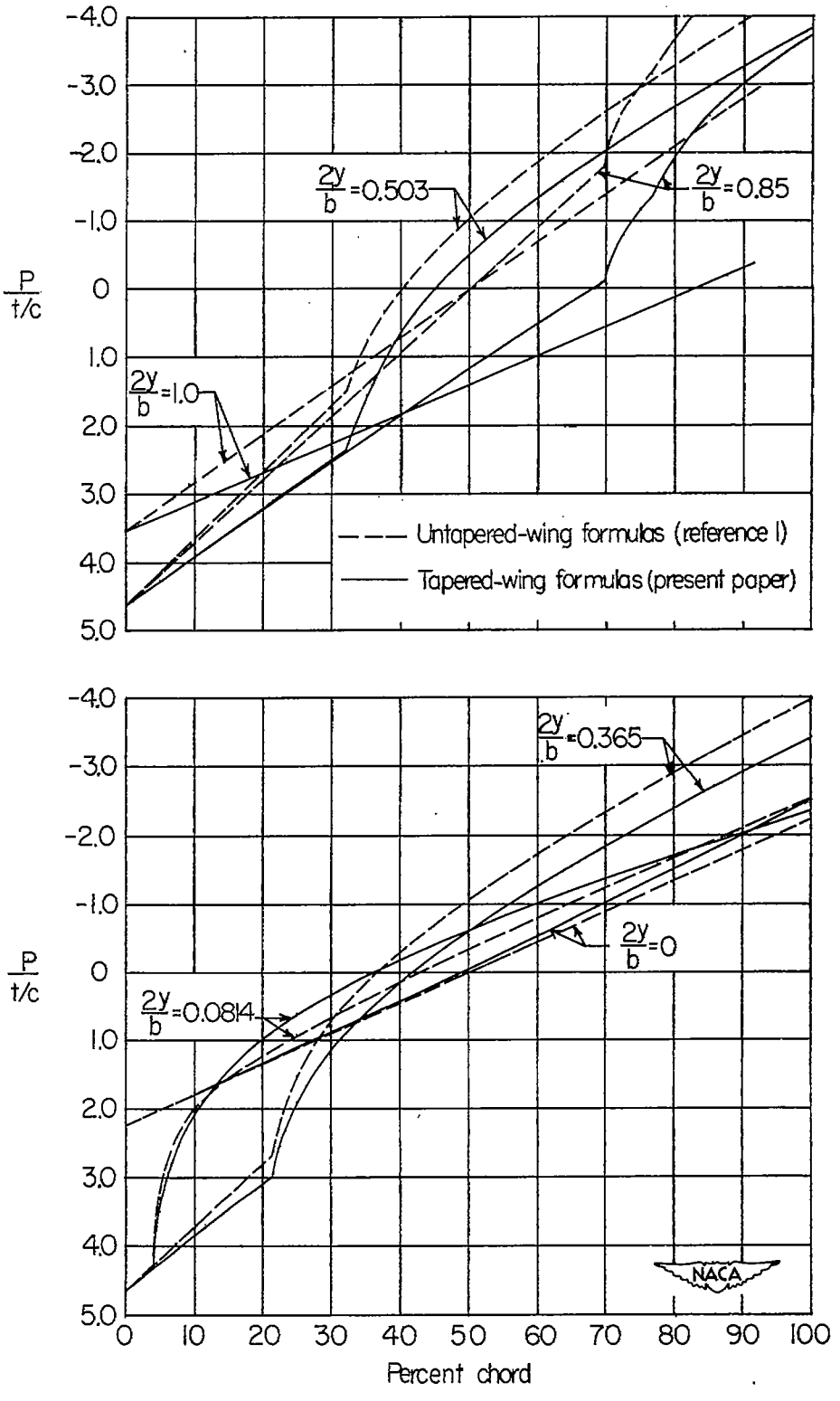

Figure 2.- Illustrative chordwise pressure distribution on a symmetrical parabolic-arc section at zero lift, $m_0\beta = 1.375$.

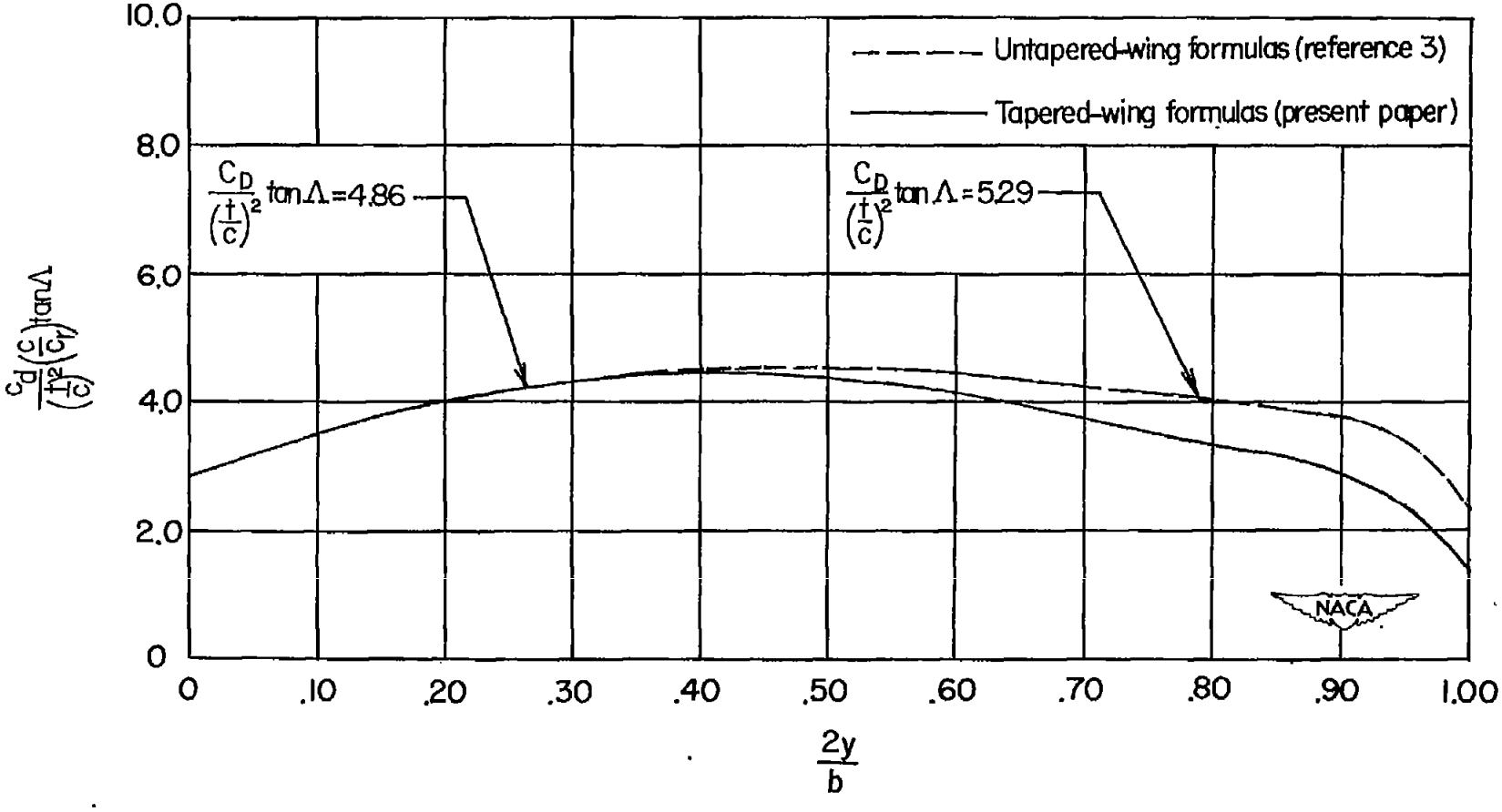

Figure 3.- Wave-drag distribution on a symmetrical parabolic-arc section at zero lift, $m_0\beta = 1.375$.

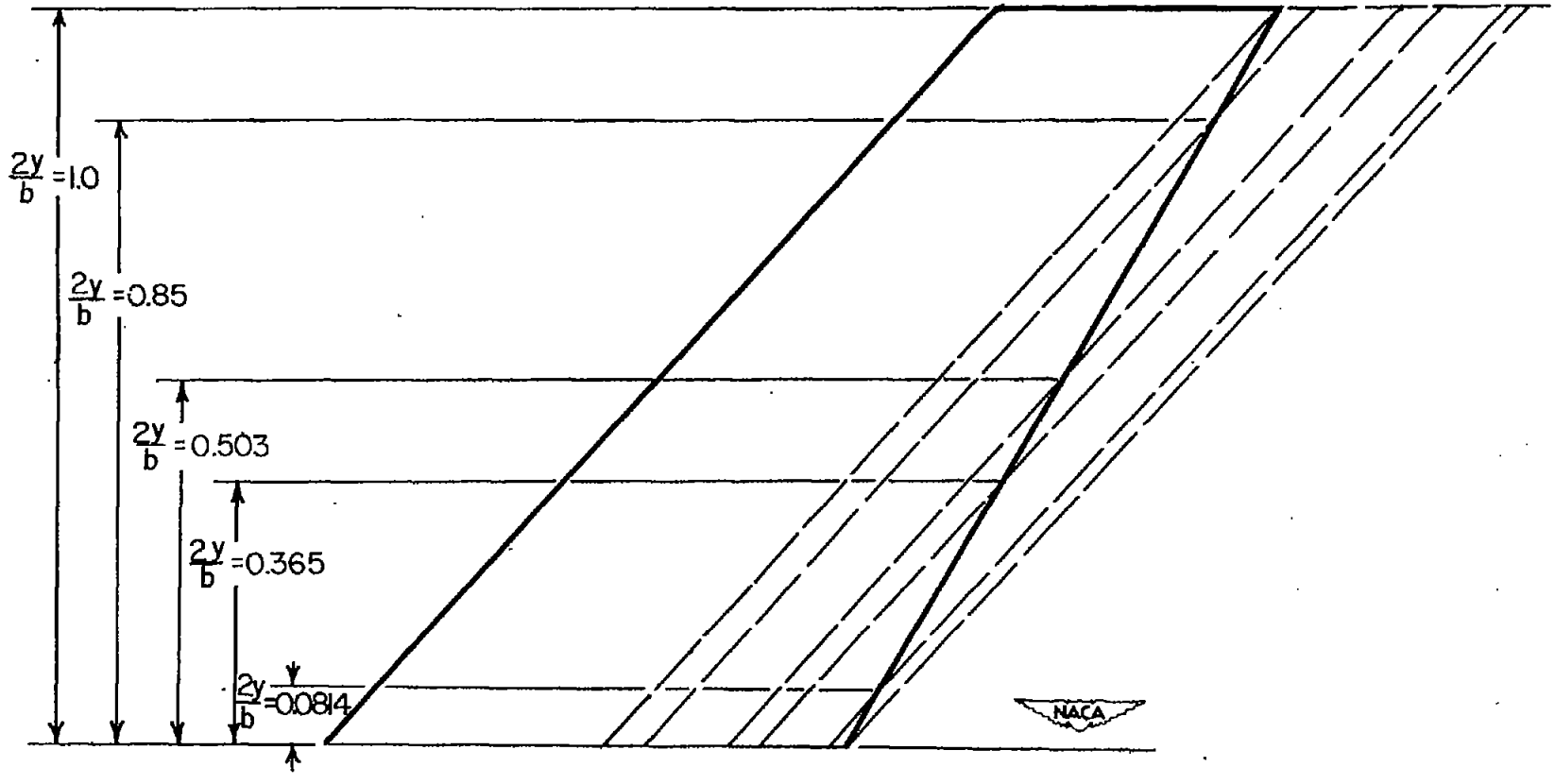

Figure 4.- Method of replacing sections of tapered wing by corresponding sections of untapered wings.

NACA-Langley - 1-8-50 - 800